

STEEP-SPECTRUM RADIO EMISSION FROM THE LOW-MASS ACTIVE GALACTIC NUCLEUS GH 10

J. M. WROBEL,¹ J. E. GREENE,² L. C. HO,³ AND J. S. ULVESTAD¹

Received 2008 June 18; accepted 2008 July 18

ABSTRACT

GH 10 is a broad-lined active galactic nucleus (AGN) energized by a black hole of mass $800,000 M_{\odot}$. It was the only object detected by Greene et al. in their Very Large Array (VLA) survey of 19 low-mass AGNs discovered by Greene & Ho. New VLA imaging at 1.4, 4.9, and 8.5 GHz reveals that GH 10's emission has an extent of less than 320 pc, has an optically thin synchrotron spectrum with a spectral index $\alpha = -0.76 \pm 0.05$ ($S_{\nu} \propto \nu^{+\alpha}$), is less than 11% linearly polarized, and is steady—although poorly sampled—on timescales of weeks and years. Circumnuclear star formation cannot dominate the radio emission, because the high inferred star formation rate, $18 M_{\odot} \text{ yr}^{-1}$, is inconsistent with the rate of less than $2 M_{\odot} \text{ yr}^{-1}$ derived from narrow H α and [O II] $\lambda 3727$ emission. Instead, the radio emission must be mainly energized by the low-mass black hole. GH 10's radio properties match those of the steep-spectrum cores of Palomar Seyfert galaxies, suggesting that, like those galaxies, the emission is outflow-driven. Because GH 10 is radiating close to its Eddington limit, it may be a local analog of the starting conditions, or seeds, for supermassive black holes. Future imaging of GH 10 at higher linear resolution thus offers an opportunity to study the relative roles of radiative versus kinetic feedback during black hole growth.

Subject headings: galaxies: active — galaxies: individual (GH 10) — galaxies: nuclei — galaxies: Seyfert — radio continuum: galaxies

Online material: color figure

1. MOTIVATION

Although little is known about the mass function of nuclear black holes with mass below about $10^6 M_{\odot}$, this is an important regime for several reasons. For example, the remarkable correlation between host bulge velocity dispersion and black hole mass strongly hints that black holes play an essential role in galaxy evolution (Kormendy 2004), yet there are few observational constraints on the starting conditions, or so-called seeds, for the supermassive black holes with masses above about $10^6 M_{\odot}$. Also, until the *Laser Interferometer Space Antenna* launches, an understanding of the low-mass end of the black hole mass function may provide one of the few constraints on these seed black holes (Hughes 2002). Moreover, it remains to be established whether small galaxies can commonly host nuclear black holes and, if so, whether the same mass versus dispersion relation mentioned above is obeyed.

Motivated by these and similar issues, Greene & Ho (2004) conducted the first systematic search for a population of black holes with mass below about $10^6 M_{\odot}$. They used SDSS DR1 to select a sample of broad-lined active galactic nuclei (AGNs) with virial mass estimates 10^5 – $10^6 M_{\odot}$. This sample of 19 objects was the first uniformly selected sample of low-mass AGNs. The sample is characterized by Eddington ratios, $L_{\text{bol}}/L_{\text{Edd}}$, that are close to unity, implying radiatively efficient accretion onto these black holes. With its low-mass black holes and high Eddington ratios, this sample probes a poorly explored region of parameter space, potentially providing new insights into the physical drivers of radio properties in AGNs. For this reason, Greene et al. (2006) observed the sample at 4.9 GHz with the Very Large Array (VLA). A single object, GH 10, was detected with a 4.9 GHz to optical flux ratio $R \sim 2.8$, formally radio-quiet (Kellermann et al.

1989). A stacked image of the remaining 18 objects yielded an upper limit of $R \leq 0.27$, emphasizing the atypical traits of GH 10.

To help understand the physical origin of these atypical traits, new multifrequency VLA data were obtained on GH 10 and are presented in § 2. As summarized in § 3.1, the radio emission from GH 10 is found to be compact, steep-spectrum, unpolarized, and steady in time. A star formation origin for this emission is considered, and dismissed, in § 3.2, while § 3.3 explores the implications of a black hole origin for the radio emission. The paper ends, in § 4, with a summary of the key findings and suggestions for future directions.

The following cosmological parameters are assumed: $H_0 = 71 \text{ km s}^{-1} \text{ Mpc}^{-1}$, $\Omega_m = 0.27$, and $\Omega_{\Lambda} = 0.75$ (Spergel et al. 2003), leading to a luminosity distance of 363 Mpc (Greene & Ho 2004; Greene et al. 2006). Also, the sign convention adopted for the spectral index α near a frequency ν is the flux density $S_{\nu} \propto \nu^{+\alpha}$.

2. VLA IMAGING

The VLA⁴ was used in the A configuration (Thompson et al. 1980) to observe GH 10 under proposal code AG745 on UT 2007 June 18 and 2007 July 15. Observations were phase-referenced to the calibrator J1224+0330 whose positional accuracy was $0.01''$. The switching angle was 5° , while the switching times were 560, 260, and 200 s for observations at center frequencies of 1.4000, 4.8601, and 8.4601 GHz, respectively. These frequencies will be abbreviated as 1.4, 4.9, and 8.5 GHz hereafter. The a priori pointing position for GH 10 was centered $3''$ south of the SDSS position (Greene & Ho 2004) to avoid any phase-center artifacts. Observations were made assuming a coordinate equinox of 2000. Data were acquired with a bandwidth of 100 MHz for each circular polarization. Observations of 3C 286 were used to set the amplitude scale to an accuracy of about 3%.

¹ National Radio Astronomy Observatory, P.O. Box O, Socorro, NM 87801; jwrobel@nrao.edu, julvesta@nrao.edu.

² Department of Astrophysical Sciences, Princeton University, Princeton, NJ 08544; jgreene@astro.princeton.edu.

³ The Observatories of the Carnegie Institution of Washington, 813 Santa Barbara Street, Pasadena, CA 91101; lho@ociw.edu.

⁴ Operated by the National Radio Astronomy Observatory, which is a facility of the National Science Foundation, operated under cooperative agreement by Associated Universities, Inc.

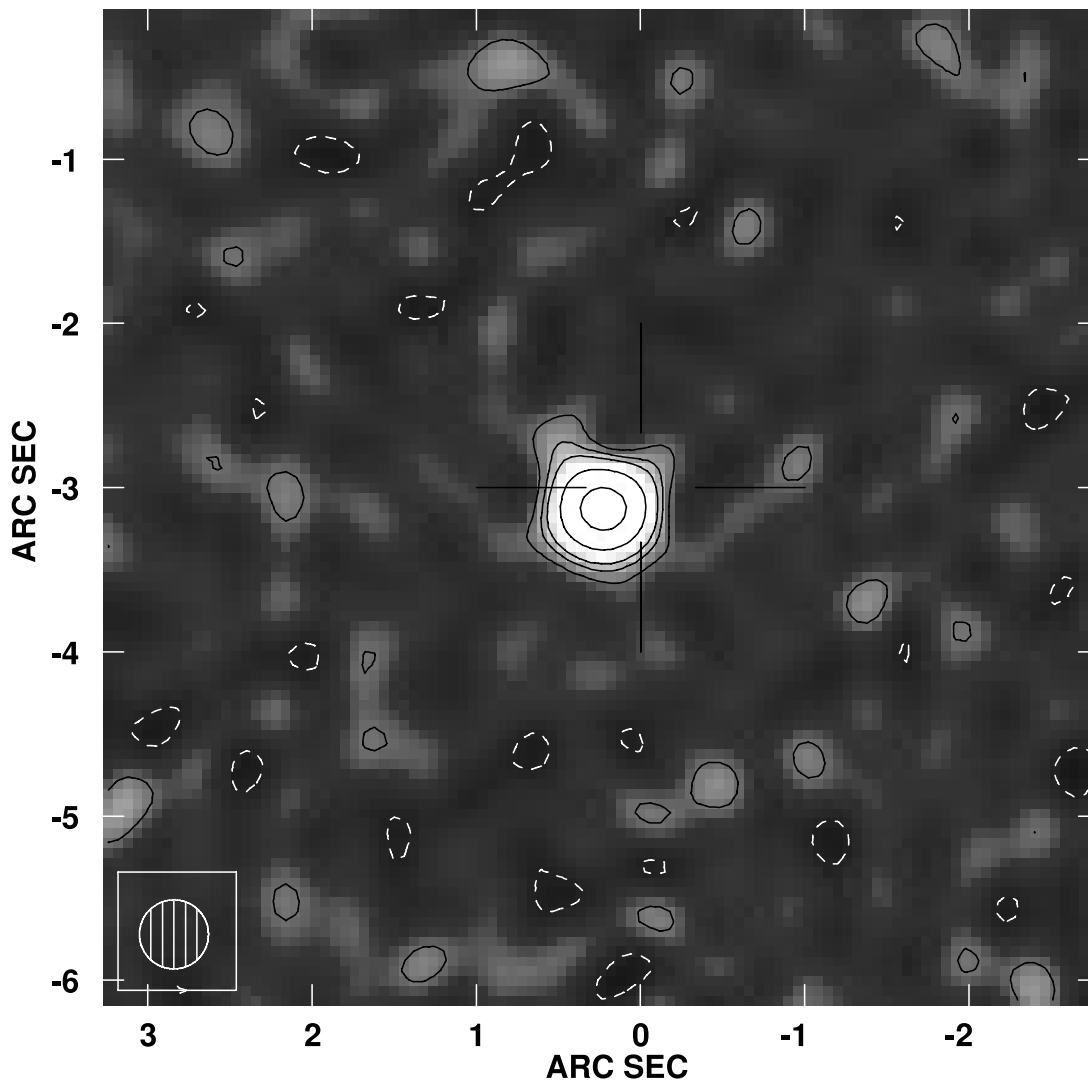


FIG. 1.—VLA image of Stokes I emission from GH 10 at a frequency of 4.9 GHz and spanning $6''$ (9 kpc). Coordinate labels are relative to the pointing position, which was centered $3''$ south of the SDSS position to avoid phase-center artifacts. SDSS position is marked with a cross with a gap. The weighting scheme used gave an rms noise of $0.022 \text{ mJy beam}^{-1}$ (1σ) and Gaussian beam dimensions at FWHM of $0.42''$ (hatched circle). Contours are at $-6, -4, -2, 2, 4, 6, 12,$ and 24 times 1σ . Negative contours are dashed and positive ones are solid. Linear color scale spans -0.1 to $0.2 \text{ mJy beam}^{-1}$. [See the electronic edition of the *Journal* for a color version of this figure.]

On 2007 June 18, net exposure times were 1500, 7800, and 8300 s at 1.4, 4.9, and 8.5 GHz, respectively. Twenty-five to 27 antennas provided data of acceptable quality, with most of the data loss attributable to EVLA retrofitting activities. The observations at 1.4 GHz were made at a large hour angle and were followed by alternating observations at 4.9 and 8.5 GHz to sample similar hour angles. On 2007 July 15, 1.4 GHz observations were made at transit and resulted in a net exposure time of 2800 s. Twenty-four antennas provided data of acceptable quality, with most of the data loss attributable to EVLA retrofitting activities and software failures. The data were calibrated using the 2007 December 31 release of the NRAO AIPS software. No self-calibrations were performed. No polarization calibration was performed, as only upper limits to the linear polarization percentages were sought. The AIPS task `imagr` was used to form and deconvolve images of the emission from GH 10.

Following Wrobel (2000), `imagr` was used to form and deconvolve Stokes I images at 4.9 and 8.5 GHz at a matched resolution at FWHM of $0.42''$. This led to detections of a compact source at both frequencies, with no evidence for adjacent emission on larger scales. The 4.9 GHz image appears in Figure 1.

Quadratic fits in the image plane yielded the integrated flux densities and the two-point spectral index given in Table 1. These flux densities from 2007 June 18 are plotted in Figure 2. The image fits also yielded identical deconvolved diameters of less than $0.21''$, as well as almost identical positions. The 4.9 GHz position is $\alpha = 12^{\text{h}}40^{\text{m}}35.825^{\text{s}}$ and $\delta = -00^{\circ}29'19.53''$ (J2000.0), with a one-dimensional error of $0.1''$, the quadratic sum of terms due to the signal-to-noise ratio (S/N) of the detection (less than $0.01''$), the phase-calibrator position error ($0.01''$), and the phase-referencing strategies (estimated to be $0.1''$). This 4.9 GHz position is consistent with the SDSS position (Greene & Ho 2004) marked in Figure 1. The `imagr` task was also used to form matched-resolution images of Stokes Q and U at 4.9 and 8.5 GHz. Those images led to no detections, with the most constraining upper limit to the linear polarization percentage being less than 11% at 4.9 GHz.

Following Ho & Ulvestad (2001), `imagr` was used in a two-step approach to form and deconvolve Stokes I images at 1.4 GHz. First, a search for confusing sources was done by using the inner array baselines to image, at low resolution, the primary antenna beam to the half-power point. Second, all array baselines were used to image GH 10 and its confusing sources, simultaneously

TABLE 1
VLA PHOTOMETRY OF GH 10

Date (1)	Resolution (arcsec) (2)	Position Angle (deg) (3)	ν (GHz) (4)	S_ν (mJy) (5)	Figure 2 (6)
2007 Jun 18	0.42, 0.42	0	4.9	0.75 ± 0.05^a	Yes
	0.42, 0.42	0	8.5	0.44 ± 0.03^a	Yes
	1.96, 1.44	-47	1.4	1.80 ± 0.09^b	Yes
	1.96, 1.44	-47	4.9	0.72 ± 0.04^b	No
2007 Jul 15	1.45, 1.36	47	1.4	1.88 ± 0.13	No

NOTES.—Col. (1): UT observation date. Cols. (2) and (3): Elliptical Gaussian resolution at FWHM and its elongation position angle. Col. (4): Center frequency. Col. (5): Flux density with error given by the quadratic sum of the 3% scale error and the 1σ rms of the fit. Col. (6): Plotted in Fig. 2?

^a Two-point spectral index $\alpha = -0.97 \pm 0.17$.

^b Two-point spectral index $\alpha = -0.73 \pm 0.06$.

and at a high resolution of about $1.4''$ at FWHM. From the GH 10 data acquired at transit on 2007 July 15, this approach led to a high-resolution image mildly affected by confusion, showing a compact detection plus no evidence for adjacent emission on larger scales; a quadratic fit in the image plane yielded the integrated flux density in Table 1 and a deconvolved diameter of less than $0.72''$. From the GH 10 data acquired at a large hour angle on 2007 June 18, the high-resolution image was more degraded by confusion so only a parabolic fit in the image plane was made. This yielded the peak flux density in Table 1 that is plotted in Figure 2. That figure also shows the spectral index $\alpha = -0.76 \pm 0.05$ derived from all the photometry on 2007 June 18.

Finally, the 4.9 GHz data were used to produce an image at the FWHM resolution of the 1.4 GHz data on 2007 June 18. A parabolic fit to that 4.9 GHz image gave the flux density listed in Table 1, leading in turn to the tabulated spectral index between 1.4 and 4.9 GHz. Also, that 4.9 GHz flux density is consistent with the value obtained at a FWHM resolution of $0.42''$ implying no additional emission on scales between $0.42''$ and about $1.4''$.

3. IMPLICATIONS

3.1. Radio Properties

The new VLA data imply that the emission from GH 10 is compact, with a diameter of less than $0.21''$ (320 pc) at 4.9 GHz (Fig. 1) and 8.5 GHz, and less than $0.72''$ (1.1 kpc) at 1.4 GHz. These upper limits are derived from data with S/Ns of 15 or more. The new 1.4 GHz images show only a compact component and do not confirm the prior hint from low-S/N data of marginally resolved emission with a FWHM diameter of $5''$ (7.5 kpc; White et al. 1997).⁵ Similarly, the new 4.9 GHz image does not confirm the prior suggestion from low S/N-data of marginally resolved emission with a FWHM diameter of $0.3''$ (530 pc; Greene et al. 2006).

The emission from GH 10 has a steep radio spectrum, with a three-point spectral index of $\alpha = -0.76 \pm 0.05$ measured on 2007 June 18 and thus free from concerns about time variability (Fig. 2). This spectral index agrees with the two-point, matched-resolution spectral indices given in Table 1, as is expected for compact, unresolved emission. The single-epoch radio spectrum shown for GH 10 in Figure 2—the first ever measured for any of the 19 low-mass AGNs discovered by Greene & Ho (Greene & Ho 2004; Greene et al. 2006)—is consistent with optically thin synchrotron emission. This emission is less than 11% linearly polarized at 4.9 GHz, well below the 73% expected for electrons with a power-law energy distribution, with index $p = 1 - 2\alpha$, in a uniform magnetic field (Shu 1991 page 197). Faraday depth effects could also be at play.

Variability timescales for AGNs are expected to scale with black hole mass (e.g., Edelson & Nandra 1999), and have not yet been explored for any of the 19 low-mass Greene & Ho objects. The new VLA photometry can be used to assess GH 10's time variability, for future comparison with other GH 10 timescales to search for physical linkages. Using only A-configuration data, the ratio of the 4.9 GHz flux density on 2007 June 18 (0.75 ± 0.05 mJy) to that on 2004 October 9 (0.7 ± 0.1 mJy; Greene et al. 2006) is $7\% \pm 16\%$, consistent with steady emission on timescales of years. The ratio of the 1.4 GHz flux density on 2007 July 15 (1.88 ± 0.13 mJy) to that on 2007 June 18 (1.80 ± 0.09 mJy) is $4\% \pm 9\%$, also consistent with steady emission on timescales of weeks. Also, folding in the B-configuration survey of White et al. (1997) the 1.4 GHz flux density of GH 10 on 1998 August 11 was 1.16 ± 0.16 mJy (peak) and 1.29 ± 0.16 mJy (integrated). For such a low-S/N and compact source, de Vries et al. (2004)

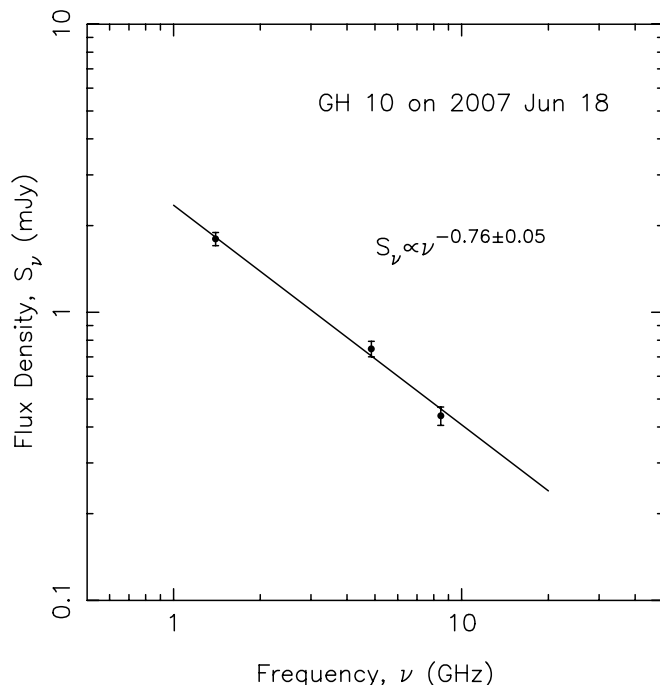


FIG. 2.—VLA spectrum of GH 10 as measured at 1.4, 4.9, and 8.5 GHz on 2007 June 18.

⁵ See <http://sundog.stsci.edu/top.html>.

advocate using the peak flux density and seeking variability at the 4σ , or greater, level. For GH 10, the ratio of the flux density on 2007 July 15 (1.88 ± 0.13 mJy) to that earlier peak (1.16 ± 0.16 mJy) is $62\% \pm 16\%$, a change of less than 4σ on a timescale of almost a decade.

In summary, the radio emission from GH 10 is compact, steep-spectrum, unpolarized, and steady—although sparsely sampled—on timescales of weeks and years. The integrated 1.4 GHz flux density corresponds to a power of 3.0×10^{22} W Hz⁻¹, while that at 4.9 GHz corresponds to a power of 1.2×10^{22} W Hz⁻¹.

3.2. Radio Emission from Star Formation?

The radio emission from GH 10 might be driven, in part, by circumnuclear star formation. Applying *scanpi* to *Infrared Astronomical Satellite* data at 60 μ m, GH 10 is undetected with a 3σ upper limit of 0.15 Jy. Equation (2) of Yun et al. (2001) yields an upper limit to the 60 μ m power. Inserting that limit into the radio-infrared relation in equation (4) of Yun et al. (2001) sets an upper limit of $<1.9 \times 10^{22}$ W Hz⁻¹ to the 1.4 GHz power expected from any star formation. This limit is below the observed power of 3.0×10^{22} W Hz⁻¹, but not by much.

A more telling analysis follows from consideration of the host galaxy's properties, especially as they relate to estimates for a star formation rate. Keck spectroscopy, with a 1'' (1.5 kpc) aperture, exhibit the Mg I *b* and Ca II infrared triplets characteristic of an old stellar population (Barth et al. 2005). *Hubble Space Telescope B* and *I* imaging, with a resolution at FWHM of 0.12'' (170 pc), reveals a smooth, spheroidal-looking system with a steep Sérsic index $n = 4$ and a color $B - I = 2$ that is characteristic of Sa or spheroidal galaxies (Greene et al. 2008). SDSS spectroscopy with a 3'' (4.5 kpc) aperture shows narrow H α and [O II] $\lambda 3727$ lines, but, as a Balmer decrement could not be robustly measured, an estimate of the internal reddening is unavailable for GH 10 (Greene & Ho 2004). However, if the average reddening advocated for the 19 Greene & Ho objects by Greene et al. (2008) is adopted and the reddening curve of Cardelli et al. (1989) is applied, then the correction factors for narrow H α and [O II] $\lambda 3727$ are 1.3 and 1.7, respectively. Then using equations (2) and (3) of Kennicutt (1998) those corrected line luminosities for GH 10 each imply a star formation rate no higher than $2 M_{\odot} \text{ yr}^{-1}$. These rate estimates are, by construction, upper limits because they neglect the portion of the line-emitting gas that is energized by the AGN rather than by star formation. Moreover, in order for GH 10 to be within the 2σ range of the radio-infrared relation mentioned above, the reddening at H α would need to be 2 mag, far more than the average (0.3 mag) and largest (0.5 mag) reddening advocated for the Greene & Ho objects (Greene et al. 2008). Fortunately, GH 10 is also detected in a *Spitzer* IRS spectrum, boding well for a future estimate of a star formation rate that is less affected by reddening concerns (C. E. Thornton et al., in preparation).

For comparison, using equation (13) of Yun et al. (2001) the observed 1.4 GHz power of GH 10 would correspond to a star formation rate of $18 M_{\odot} \text{ yr}^{-1}$. Such a high rate is clearly inconsistent with the line-based upper limit of $2 M_{\odot} \text{ yr}^{-1}$ derived above. Circumnuclear star formation cannot, therefore, dominate the radio emission from GH 10.

3.3. Radio Emission from the AGN

Based on the above analysis, it seems plausible that the radio emission from GH 10 is mainly energized by its low-mass black hole. GH 10 is radiating at about twice its Eddington luminosity, with this estimate being uncertain by a factor of 3 (Greene & Ho 2004). Thus comparisons of GH 10 with other broad-lined AGNs

with near-unity Eddington ratios are especially apt. The 4.9 GHz to optical flux ratio for GH 10 implies $R \sim 2.8$, so GH 10 is radio-quiet (Kellermann et al. 1989), a trait shared by most quasars at $z < 0.5$ (Ho & Peng 2001; Greene & Ho 2004; Greene et al. 2006). There is also a faint, compact *Chandra* detection within 1'' (1.5 kpc) of the SDSS position of GH 10, and its spectral properties resemble those of high-mass black holes (Greene & Ho 2007a). The ratio of the 4.9 GHz luminosity, 5.9×10^{38} ergs s⁻¹, to the hard X-ray luminosity, 1.9×10^{42} ergs s⁻¹, implies $R_X = 10^{-3.5}$ (Terashima & Wilson 2003). Such a value is also consistent with the values shown by most $z < 0.5$ quasars and by most luminous Seyfert 1 galaxies (Ho 2008). Unfortunately, such systems are too faint and too distant to be resolved on subkiloparsec scales in VLA images, so no structural comparisons can be made.

GH 10's values for R and R_X , plus its radio and hard X-ray luminosities, also resemble those for the more luminous Palomar Seyfert galaxies (Panessa et al. 2007). VLA imaging at 1.4 and 4.9 GHz of the Palomar Seyfert galaxies, with a resolution of about 1'' (100 pc at the median distance of 20 Mpc), shows a wide range of radio powers (10^{18} – 10^{25} W Hz⁻¹), spectral indices (+0.5 to -1), and linear sizes (a few tens of parsecs to 15 kpc) (Ho & Ulvestad 2001; Ulvestad & Ho 2001). Their structures mainly show a compact core, either unresolved or slightly resolved, sometimes with adjacent elongated, jetlike/outflow components. Linearly polarized emission, while rarely detected, is preferentially associated with features adjacent to the cores. Thus GH 10's radio properties most resemble those of the steep-spectrum cores of the Palomar Seyfert galaxies, for which the emission is unmodified by the effects of internal and/or external opacity. Like the Palomar Seyfert galaxies, the steep-spectrum emission from GH 10 could be outflow-driven. Moreover, the lower escape velocity from GH 10's dwarf host galaxy (Barth et al. 2005) would make it easier for any synchrotron-emitting plasma to leave the vicinity of the AGN, thereby favoring a steep, rather than flat or inverted, radio spectrum.

This work has established that the radio emission from GH 10 is compact, steep-spectrum, unpolarized, and steady. Still, GH 10 is known to be atypical when compared to the other GH objects, which are especially radio-quiet with $R \leq 0.27$ from a stacking analysis (Greene et al. 2006). Following those authors, by analogy with supermassive and stellar-mass black holes, a near-unity Eddington ratio suggests that the low-mass black hole GH 10 is presently in the very high state, with its entry into that state from the high/soft state accompanied by an optically thin ejection event in the radio. Within this framework, and barring opacity effects, the radio emission from GH 10 would be the slowly fading, steep-spectrum remnant from that ejection event, whose power corresponds to the quenched radio levels expected for the high/soft state (e.g., Maccarone et al. 2003). Also, a radio detection of only one of the 19 GH objects suggests, at face value, that such radio ejections from GH objects occur only about 5% of the time. Interestingly, a 5% duty cycle resembles that established observationally for radio flares from microquasars (e.g., Nipoti et al. 2005).

Because the low-mass black hole GH 10 is radiating close to its Eddington limit, it may be a local analog of the starting conditions, or seeds, for supermassive black holes. From the present work, the diameter of GH 10's radio emission must be less than 0.21'' (320 pc). If GH 10 is indeed driving some of this emission, then 1.4 GHz imaging with Very Long Baseline Interferometry (VLBI) at a resolution of 0.005'' (7.5 pc) will reveal the physical connection between the black hole and the synchrotron-emitting plasma. Although GH 10 is a faint radio source (Table 1), VLBI imaging of such sources is feasible (e.g., Wrobel & Ho 2006) and

would offer a means to study the relative roles of radiative versus kinetic feedback during black hole growth (e.g., Di Matteo et al. 2005; Kuhlen & Madau 2005).

4. SUMMARY AND FUTURE DIRECTIONS

GH 10 was the only object detected by Greene et al. (2006) in their VLA survey of the 19 low-mass AGNs discovered by Greene & Ho (2004). New VLA imaging reveals that the emission from GH 10 has an extent of less than 320 pc, with an optically thin synchrotron spectrum that is less than 11% linearly polarized. The radio emission is steady, although poorly sampled, on time-scales of weeks and years. Circumnuclear star formation cannot dominate the radio emission, because the inferred star formation rate, $18 M_{\odot} \text{ yr}^{-1}$, is inconsistent with the upper limit of $2 M_{\odot} \text{ yr}^{-1}$ derived from the narrow optical emission lines. Instead, the radio emission must be dominantly energized by the low-mass black hole, which is thought to be radiating near its Eddington limit.

The radio properties of GH 10 strongly resemble those of the steep-spectrum cores of Palomar Seyfert galaxies, which feature outflow-driven emission unmodified by the effects of internal and/or external opacity. This suggests that, like those Palomar Seyferts galaxies, the radio emission from GH 10 is outflow-driven, a suggestion that can be tested with future VLBI imaging. Such imaging could also offer an opportunity to study the relative roles of radiative versus kinetic feedback during black hole growth, given that GH 10 may be a local analog of the starting conditions, or seeds, for supermassive black holes. Finally, the compact, steep-spectrum, unpolarized, and steady nature of the emission from GH 10 will guide future observations of the new 1.4 GHz detections of low-mass AGNs reported by Greene & Ho (2007b).

We acknowledge useful feedback from an anonymous referee.

Facilities: VLA

REFERENCES

- Barth, A. J., Greene, J. E., & Ho, L. C. 2005, *ApJ*, 619, L151
 Cardelli, J. A., Clayton, G. C., & Mathis, J. S. 1989, *ApJ*, 345, 245
 de Vries, W. H., Becker, R. H., White, R. L., & Helfand, D. J. 2004, *AJ*, 127, 2565
 Di Matteo, T., Springel, V., & Hernquist, L. 2005, *Nature*, 433, 604
 Edelson, R., & Nandra, K. 1999, *ApJ*, 514, 682
 Greene, J. E., & Ho, L. C. 2004, *ApJ*, 610, 722
 ———. 2007a, *ApJ*, 656, 84
 ———. 2007b, *ApJ*, 670, 92
 Greene, J. E., Ho, L. C., & Barth, A. J. 2008, *ApJ*, in press
 Greene, J. E., Ho, L. C., & Ulvestad, J. S. 2006, *ApJ*, 636, 56
 Ho, L. C. 2008, *ARA&A*, 46, 475
 Ho, L. C., & Peng, C. Y. 2001, *ApJ*, 555, 650
 Ho, L. C., & Ulvestad, J. S. 2001, *ApJS*, 133, 77
 Hughes, S. A. 2002, *MNRAS*, 331, 805
 Kellermann, K. I., Sramek, R. A., Schmidt, M., Shaffer, D. B., & Green, R. F. 1989, *AJ*, 98, 1195
 Kennicutt, R. C., Jr. 1998, *ARA&A*, 36, 189
 Kormendy, J. 2004, in *Coevolution of Black Holes and Galaxies*, ed. L. C. Ho (Cambridge: Cambridge Univ. Press), 1
 Kuhlen, M., & Madau, P. 2005, *MNRAS*, 363, 1069
 Maccarone, T. J., Gallo, E., & Fender, R. 2003, *MNRAS*, 345, L19
 Nipoti, C., Blundell, K. M., & Binney, J. 2005, *MNRAS*, 361, 633
 Panessa, F., Barcons, X., Bassani, L., Cappi, M., Carrera, F. J., Ho, L. C., & Pellegrini, S. 2007, *A&A*, 467, 519
 Shu, F. H. 1991, *The Physics of Astrophysics*, Vol. 1., Radiation (Mill Valley: University Science Books)
 Spergel, D. N., et al. 2003, *ApJS*, 148, 175
 Terashima, Y., & Wilson, A. S. 2003, *ApJ*, 583, 145
 Thompson, A. R., Clark, B. G., Wade, C. M., & Napier, P. J. 1980, *ApJS*, 44, 151
 Ulvestad, J. S., & Ho, L. C. 2001, *ApJ*, 558, 561
 White, R. L., Becker, R. H., Helfand, D. J., & Gregg, M. D. 1997, *ApJ*, 475, 479
 Wrobel, J. M. 2000, *ApJ*, 531, 716
 Wrobel, J. M., & Ho, L. C. 2006, *ApJ*, 646, L95
 Yun, M. S., Reddy, N. A., & Condon, J. J. 2001, *ApJ*, 554, 803